

Zero Air Gap Condition in Aerostatic Flat Bearings

Original

Zero Air Gap Condition in Aerostatic Flat Bearings / Colombo, Federico; Lentini, Luigi; Raparelli, Terenziano; Viktorov, Vladimir; Trivella, Andrea - In: Advances in Mechanism and Machine ScienceELETTRONICO. - [s.l.] : Springer International Publishing, 2019. - ISBN 978-3-030-20131-9. - pp. 3929-3937

Availability:

This version is available at: 11583/2738254 since: 2020-11-12T11:44:24Z

Publisher:

Springer International Publishing

Published

DOI:

Terms of use:

This article is made available under terms and conditions as specified in the corresponding bibliographic description in the repository

Publisher copyright

Springer postprint/Author's Accepted Manuscript

(Article begins on next page)

Zero Air Gap Condition in Aerostatic Flat Bearings

Federico Colombo¹, Luigi Lentini^{1*}, Terenziano Raparelli¹, Vladimir Viktorov¹,

Andrea Trivella¹

¹ Politecnico di Torino, Turin (TO) 10129, Italy

* luigi.lentini@polito.it

Abstract. In the last fifty years, the performance of aerostatic pads has been largely investigated as regards load capacity, consumption, stiffness and damping. However, there are few works studying the effect of other aspects which are not usually taken into account, e.g., deformations, waviness and roughness. This paper investigates the causes of air leakages at zero air gap condition. Different numerical simulations are performed to evaluate which is the deformed shape of the pad under different loading conditions. Experimental air flow measurements at zero air gap condition were also performed. It has been found that, in this instance, pad deflection is one of the main causes producing air leakages.

Keywords: air bearing, gas bearing, aerostatic pads, lubrication.

1 Introduction

Because of their outstanding features, aerostatic bearings are widely used in different high precision industrial applications, e.g., metrology, nuclear, biomedical and manufacturing [1]. The low viscosity of air allows relative motion with almost zero friction and wear.

Large number of studies have been performed to understand which are the key aspects that have to be taken into account for the aerostatic bearing design. The selection of the bearing feeding system is one of the most crucial aspect. Feeding compensation allows the variation of the air gap height when the load supported by bearings change. The most common feeding systems are simple orifices, pocketed orifices, micro holes, porous surfaces and compound restrictors. The performance of aerostatic bearings with simple and pocketed orifices were the first to be investigated. In these instances, the influence of the recess shape and dimension, supply pressure, supply hole diameter and position were largely investigated. Boffey et al. [2, 3] performed an experimental study on the effect of the supply pressure and the orifice size over the performance of air lubricated bearings with pocketed orifices. Chen and He [4] demonstrated also that the recess shape have a significant effect of the pad performance. They found that that spherical and rectangular recesses can generate vortexes which can compromise bearing performance. Colombo et al. [5] performed a numerical and experimental study of the static and dynamic performance aerostatic rectangular pads with multiple simple orifices. They investigated the effect of the supply pressure and supply hole diameter

on the pad performance, eventually performing a sensitivity analysis to find an optimal supply hole location. To increase the relatively low stiffness and poor damping of aerostatic bearings, porous surface, compound restrictors and micro holes were experimented as feeding systems. Fourka and Bonis [6] compared the performance of porous pads to those of pads with discrete number of restrictors. They highlighted the remarkable influence of the permeability of the adopted porous surfaces. Yoshimoto and Khinno [7] studied the performance of porous aerostatic bearings with a groove air supply and a hole air supply to find a technical solution to reduce the deflection of porous surfaces. Despite the higher performance, the main problem in the use of porous surfaces is the selection of the porous material that must exhibit suitable permeability and strength [8]. Another way to obtain aerostatic bearings with higher performance is the use of compound restrictors. Compound restrictors consist in simple restrictors surrounded by grooves with different geometries. The groove insertion usually enhances the bearing stiffness and load carrying capacity generating a more uniform air gap pressure distribution. Colombo et al. [9–13] studied the static and dynamic performance of rectangular aerostatic pads with different groove configurations. Charki et al. [14] performed numerical and experimental studies of the performance of circular aerostatic pads with multiple orifices. The use of micro holes is the last type of feeding system that has been experimented thanks to the recent innovations in laser technology. Belforte et al. [15] performed numerical and experimental studies on aerostatic pads with micro holes by providing an empirical formula to compute their discharge coefficients. Mitayake et al. [16] compared the performance of aerostatic pads with small feed holes to that of compound restrictors by finding that they provide similar stiffness similar and higher damping coefficient.

Despite literature presents a large number of investigations on aerostatic bearing, there is a lack of numerical and experimental works considering the effect of pads material, leakages and macro and micro geometrical errors. Lu et al. [17] developed a FEM model considering the fluid-structure interactions to evaluate the effect deformations over the bearing performance. They found that, in some instances, air gap pressure distribution may generate significant deformations of the pad.

In most of the cases, externally pressurized pads may exhibit air leakages even when they are in contact with the counter surface.

The aim of this work is to shed light on the causes of this phenomenon.

2 The Aerostatic Pad

The pad employed in this investigation is an Aluminum rectangular pad with size of $75 \times 50 \text{ mm}^2$ and thickness equal to 13 mm. Figure 1 shows a photograph of the active surface of the pad. The pad presents eight supply holes with a diameter of 0.2 mm which are distributed on a supply rectangle of size $55 \times 30 \text{ mm}^2$.



Fig. 1. Photograph of the investigated pad.

For further details, the static and dynamic performance of these pads was investigated in [5].

3 Experimental Set-up

Figure 2 shows the testing configuration adopted to carry out the campaign of air flow measurements. The pneumatic circuit at the upstream of the pad is composed of a regulator valve (1), a bistable 3/2 pneumatic valve with manual control (2), a variable pneumatic resistance (3), a flowmeter (4) and a digital pressure transducer (5).

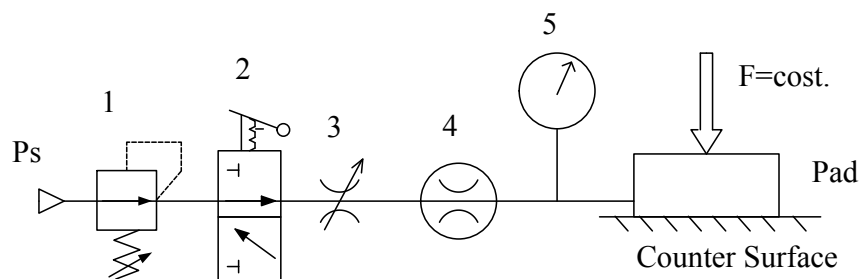


Fig. 2. The adopted testing configuration.

The pressure regulator (1) is used to set the supply pressure of the pad. The pneumatic valve (2) is used to rapidly connect the circuit to the supply or to the vent. The pneumatic variable resistance (3) is necessary to obtain a second and finer regulation of the pad supply pressure. The flowmeter (4) and the digital pressure transducer measure the air mass flow rate and the supply pressure of the pad.

4 Methodology

The aim of the described methodology is to investigate the presence of air leakages when the air pad is in contact with its counter surface with a preload higher than its maximum load capacity. The main hypothesis at the base of this campaign of experiments is that air leakages are essentially due to the pad deflection and to the roughness of the mating surfaces. Here, only the effect of the pad deflection is investigated. Two numerical simulations were performed to clarify which is the deformed shape of the pad when it is subjected to the external loads. The first simulation consists in a contact analysis to investigate the effect of the external load with no supply air. The second simulation is aimed to reproduce the conventional working condition of the pad, i.e., the simultaneous presence of an external load and an air pressure distribution. This configuration was modelled by considering a constant pressure distribution under the pad which is balanced by the external load. Table 1 summarizes the material properties which were employed in the simulations:

Table 1. Material properties of pad and countersurface.

| | Young Modulus E [MPa] | Poisson ratio ν [-] |
|-------------|-----------------------|-------------------------|
| Pad | 70 000 | 0.3 |
| Counter Pad | 210 000 | 0.3 |

The second part of the study consists in experimental tests to measure the air leakages when the pad is in contact with its counter surface. To ensure the presence of a solid-to-solid contact, the pad was loaded with a force (1200 N) higher than the maximum load capacity of the pad. The test consists in measuring the air leakages as a function of the supply pressure.

5 Results

5.1 Numerical Simulations

Figure 3 shows the results of a numerical simulation performed to evaluate the pad deformations due to the external load only ($F= 1200$ N). This loading condition was simulated through a 2D FEM contact analysis considering the symmetry of the problem. The simulation demonstrates that, in the absence of an air gap pressure distribution under the pad, the external load induced negligible pad deformations. It is possible to see that the loading tip deforms the pad locally, but does not modify its shape.

The second simulation was performed to evaluate the deformed shape of the pad when it is subject to an external load balanced by the pressure distribution that establishes in the gap under the pad. Figure 4 shows the field of displacement and the deformed shape of the pad in this second configuration. It is possible to see that, in this instance, since the active surface of the pad becomes convex, the pad deflection is no more negligible.

This means that, the simultaneous presence of external loads and air gap pressure distributions significantly deflects the active surface of the pad thus generating air leak-ages. Figure 5 shows the deformed profile shape of the upper surface of the pad obtained with loads ranging from 100 to 800 N.

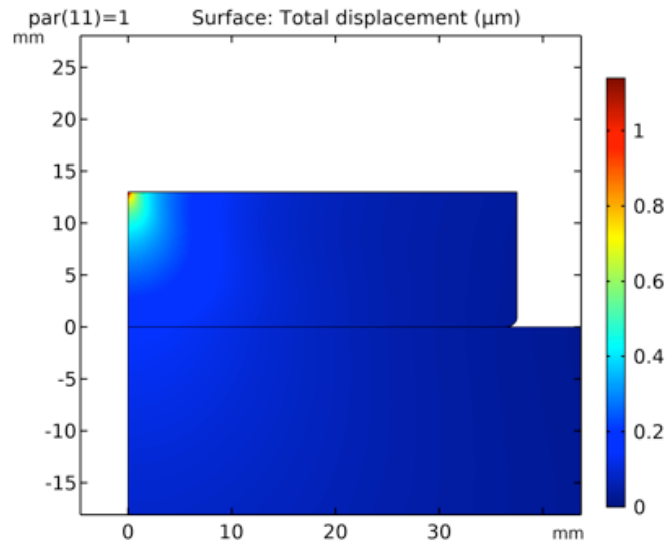


Fig. 3. Results from the numerical simulation performed to evaluate the pad deformations due to the external load only ($F= 1200$ N).

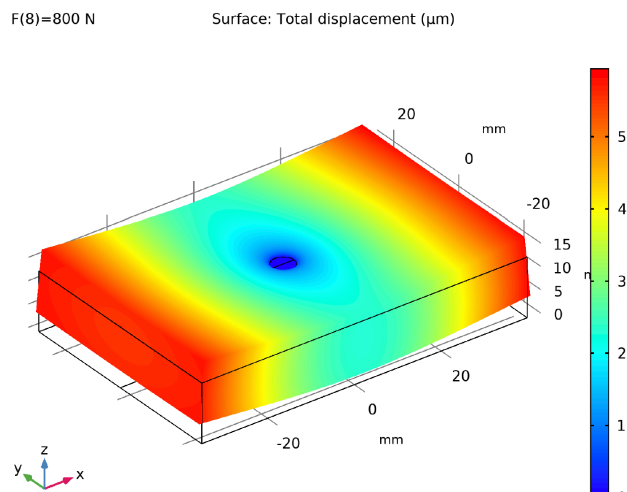


Fig. 4. Deformed shape of the pad due to the external load and the pressure establishes in the air gap.

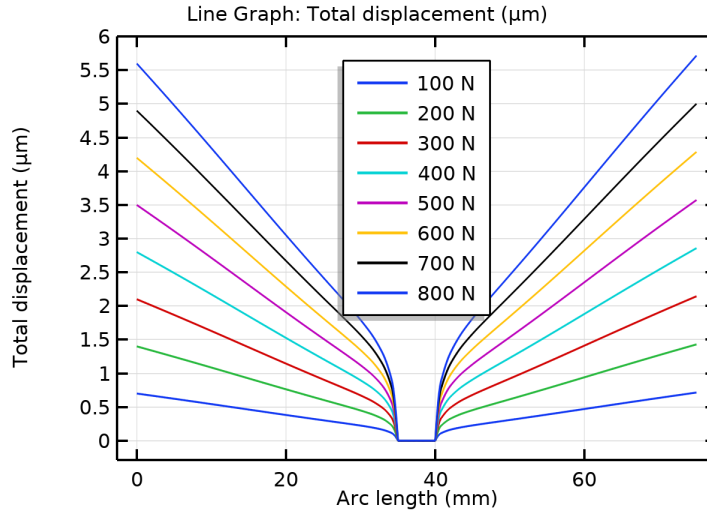


Fig. 5. Deformed shape of the upper surface profile of the pad in the presence of different loading conditions.

5.2 Air Flow Measurements

Figure 6 shows the results of the air flow measurements performed by modifying the supply pressure of the pad in the presence of a constant external load of 1200 N. The expression of the air flow through a rectangular duct was employed to evaluate the correspondent equivalent air gap:

$$G = \frac{h^3 (P_{in}^2 - P_{out}^2)}{24\mu RT} \frac{b}{l} \quad (1)$$

where, h is the air gap height, P_{in} and P_{out} are the inlet and the outlet pressures, b and l are the width and length of an equivalent rectangular duct and μ , R and T are the dynamic viscosity, gas constant and temperature. It is worth pointing out that the pressure drop in the supply orifices can be neglected as the air consumption is small. Ratio b/l can be estimated from eq. (1) measuring G and knowing all other parameters.

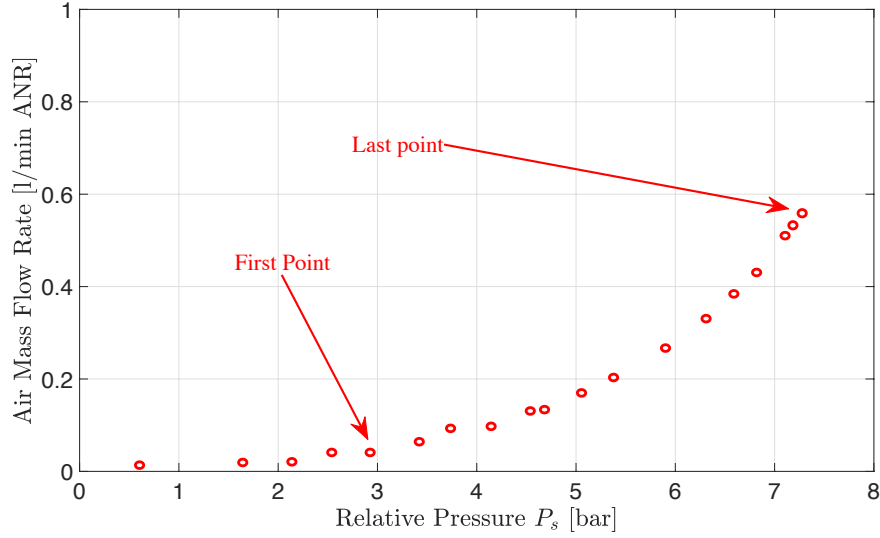


Fig. 6: Air mass flow rate expressed as a function of the supply pressure with a constant external load equal to 1200 N

The first point of the considered range (see Figure 6) was taken as reference value (P_{ref} , G_{ref}) and dimensionless air gap heights were evaluated as:

$$\bar{h} = \frac{h}{h_{ref}} = \sqrt[3]{\frac{G}{G_{ref}} \cdot \frac{P_{ref}^2 - P_a^2}{P_s^2 - P_a^2}} \quad (2)$$

Figure 7 shows the trend of the dimensionless air gap \bar{h} expressed as a function of the absolute supply pressure P_s . As it is possible to see, the computed air gap shows a linear trend even though the pad is in contact with its counter surface. This indicates that, depending on the external force and the supply pressure, pads may be subject to significant deflections that lead to air leakages. Hence, the higher is the external load and supply pressure, the poorer are the performance simulated by rigid pad models based on Reynolds' equation.

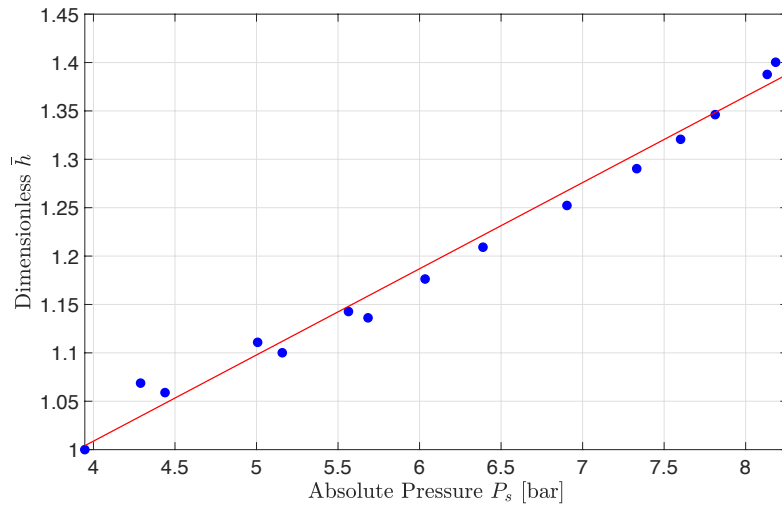


Fig. 7. Dimensionless air gap height expressed as a function of the absolute supply pressure.

6 Conclusions

This paper describes a numerical and an experimental study aimed to investigate the behavior of an aerostatic pad at zero air gap condition. The main goal is to have a better understanding of the causes of the presence of air leakages when the pad is in contact with its counter surface. In particular, this study focuses on seeking a correlation between pad deflections and air leakages. It was found that pad deflection has a large influence on the air leakages even when the pad is in contact with its counter surfaces. A dimensionless expression of the air gap height was used to evaluate how this parameter varies with the supply pressure.

7 References

1. Lentini, L., Moradi, M., Colombo, F.: A Historical Review of Gas Lubrication: From Reynolds to Active Compensations. *Tribology in Industry*. 40, 165–182 (2018). doi:10.24874/ti.2018.40.02.01
2. Boffey, D.A., Wilson, P.M.: An experimental investigation of the pressures at the Edge of a gas bearing pocket. *Journal of Lubrication Technology*. 103, 593–600 (1981)
3. Boffey, D.A., Duncan, A.E., Dearden, J.K.: An experimental investigation of the effect of orifice restrictor size on the stiffness of an industrial air lubricated thrust bearing. *Tribology International*. 14, 287–291 (1981)

4. Chen, X.-D., He, X.-M.: The effect of the recess shape on performance analysis of the gas-lubricated bearing in optical lithography. *Tribology international*. 39, 1336–1341 (2006)
5. Colombo, F., Lentini, L., Raparelli, T., Trivella, A., Viktorov, V.: Dynamic Characterisation of Rectangular Aerostatic Pads with Multiple Inherent Orifices. *Tribology Letters*. 66, (2018). doi:10.1007/s11249-018-1087-x
6. Fourka, M., Bonis, M.: Comparison between externally pressurized gas thrust bearings with different orifice and porous feeding systems. *Wear*. 210, 311–317 (1997). doi:http://dx.doi.org/10.1016/S0043-1648(97)00079-3
7. Yoshimoto, S., Kohno, K.: Static and Dynamic Characteristics of Aerostatic Circular Porous Thrust Bearings (Effect of the Shape of the Air Supply Area). *Journal of Tribology*. 123, 501 (2001). doi:10.1115/1.1308027
8. KWAN, Y.B.P., CORBETT, J.: Porous aerostatic bearings: an updated review. *Wear*. 222, 69–73 (1998)
9. Colombo, F., Lentini, L., Raparelli, T., Trivella, A., Viktorov, V.: A Lumped Model for Grooved Aerostatic Pad. In: *Advances in Service and Industrial Robotics*. pp. 678–686. Springer International Publishing (2018)
10. Colombo, F., Lentini, L., Raparelli, T., Trivella, A., Viktorov, V.: Dynamic model of a grooved thrust bearing: Numerical model and experimental validation. Presented at the AIMETA 2017 - Proceedings of the 23rd Conference of the Italian Association of Theoretical and Applied Mechanics (2017)
11. Colombo, F., Lentini, L., Raparelli, T., Viktorov, V.: Experimental Identification of an Aerostatic Thrust Bearing. In: *Advances in Italian Mechanism Science*. pp. 441–448. Springer (2017)
12. Colombo, F., Lentini, L., Raparelli, T., Viktorov, V.: Actively compensated aerostatic thrust bearing: design, modelling and experimental validation. *Mechanica*. 1–16 (2017). doi:10.1007/s11012-017-0689-y
13. Colombo, F., Lentini, L., Raparelli, T., Trivella, A., Vladimir, V.: A nonlinear lumped parameter model of an externally pressurized rectangular grooved air pad bearing. In: *Advances in Italian Mechanism Science*. pp. 490–497. Springer (2018)
14. Charki, A., Diop, K., Champmartin, S., Ambari, A.: Numerical simulation and experimental study of thrust air bearings with multiple orifices. *International Journal of Mechanical Sciences*. 72, 28–38 (2013). doi:10.1016/j.ijmecsci.2013.03.006
15. Belforte, G., Colombo, F., Raparelli, T., Trivella, A., Viktorov, V.: Experimental Analysis of Air Pads with Micro Holes. *Tribology Transactions*. 56, 169–177 (2013). doi:10.1080/10402004.2012.734547
16. Miyatake, M., Yoshimoto, S.: Numerical investigation of static and dynamic characteristics of aerostatic thrust bearings with small feed holes. *Tribology International*. 43, 1353–1359 (2010). doi:10.1016/j.triboint.2010.01.002
17. Lu, L., Chen, W., Yu, N., Wang, Z., Chen, G.: Aerostatic thrust bearing performances analysis considering the fluid-structure coupling effect. *Proceedings of the Institution of Mechanical Engineers, Part J: Journal of Engineering Tribology*. 230, 1588–1596 (2016). doi:10.1177/1350650116642098

